

See discussions, stats, and author profiles for this publication at: <https://www.researchgate.net/publication/242272860>

Electron Emission from $N(BF_3)_4^{3-}$ Hindered by a Sphere of Negative Charges

ARTICLE in THE JOURNAL OF PHYSICAL CHEMISTRY A · NOVEMBER 2001

Impact Factor: 2.69 · DOI: 10.1021/jp011764j

CITATIONS

10

READS

7

2 AUTHORS, INCLUDING:



Andreas Dreuw

Universität Heidelberg

154 PUBLICATIONS 6,753 CITATIONS

SEE PROFILE

Electron Emission from $\text{N}(\text{BF}_3)_4^{3-}$ Hindered by a Sphere of Negative Charges

A. Dreuw* and L. S. Cederbaum

Theoretische Chemie, Physikalisch-Chemisches Institut, Universität Heidelberg, Im Neuenheimer Feld 229, 69120 Heidelberg, Germany

Received: May 9, 2001; In Final Form: September 11, 2001

The unique $\text{N}(\text{BF}_3)_4^{3-}$ trianion, which is prognosticated to be the first *small* long-lived covalent gas-phase trianion in the literature so far, is theoretically examined in detail. High-level ab initio methods show that the T symmetric system is long-lived with respect to fragmentation and metastable with respect to electron emission. To estimate the lifetime of the $\text{N}(\text{BF}_3)_4^{3-}$ trianion with respect to electron emission, we have calculated the repulsive Coulomb barrier and used this potential to compute the lifetime in the framework of Wentzel–Kramer–Brioullin theory. The estimated lifetime is markedly longer than 5 μs , and we predict the $\text{N}(\text{BF}_3)_4^{3-}$ trianion to be observable in a mass spectrometer experiment. The longevity of the trianion with respect to electron emission can be explained by the unbound electrons caught in a negative charged sphere of fluorine atoms.

1. Introduction

Multiply charged anions (MCAs) are commonly observed on surfaces, in solutions, or as “building blocks” in condensed matter such as $[\text{A}^{n-}][\text{B}^{m+}]$ salts. In such chemical environments, the local electrostatic field constituted by the surrounding counterions helps stabilize the MCA with respect to fragmentation and emission of one or more of the excess negative charges. Without these stabilizing effects in the gas phase, the existence of MCAs is very unlikely due to the strong electrostatic repulsion between their excess negative charges. Indeed, this strong electrostatic repulsion is the reason that most of the well-known textbook MCAs, e.g. CO_3^{2-} ,^{1–3} SO_4^{2-} ,^{4–6} PO_4^{3-} ,⁴ and several others, instantly emit one electron when they are brought to the gas phase as isolated entities.

In contrast to the given examples of electronically unstable MCAs, several small dianions have been found experimentally and theoretically to be long-lived in the gas phase.^{7–9} Such small dianions are, for example, LiF_3^{2-} ,¹⁰ BeF_4^{2-} ,^{11–13} C_7^{2-} ,^{14,15} S_n^{2-} ,¹⁶ $\text{S}_2\text{O}_6^{2-}$,^{5,6} SiC_6^{2-} ,^{17–19} BeC_4^{2-} ,^{20,21} and PtCl_4^{2-} .^{22,23} It is worth mentioning that the theoretical prediction of the dianions BeF_4^{2-} ¹¹ and SiC_6^{2-} ¹⁸ encouraged the experimental search for these species, which has culminated in their mass spectrometric detection.^{13,19}

The stable gas-phase dianions can be generally classified into two groups. On one hand, there exist chainlike dianions whose excess electrons are localized in electron affine groups at the ends of the chain. In these systems the local binding energy of the single electrons in the electron affine subgroups exceeds the electrostatic repulsion between the excess charges. Prominent members of this group are the dianions of the aliphatic dicarboxylic acids $^-\text{OOC}-(\text{CH}_2)_n-\text{COO}^-$ ($n > 2$)^{24–26} and the chainlike polysulfide dianions S_n^{2-} ($n > 6$).¹⁶ On the other hand, there are branched or starlike dianions, which exhibit a geometrical arrangement of positive and negative charges such that the electrostatic attraction exceeds the electrostatic repulsion within these systems. This principle becomes clear when the

ionic LiF_3^{2-} dianion¹⁰ is thoroughly investigated. The LiF_3^{2-} dianion possesses a D_{3h} symmetric arrangement of a central Li^+ cation and three equivalent F^- anions. At this symmetry the electrostatic attraction between the central Li^+ cation and the F^- ligands always beats the electrostatic repulsion between the F^- ligands by a factor of $\sqrt{3}$.

Although until now several dianions are known, and their electron binding mechanisms well understood, higher than doubly charged gas-phase anions are scarce in the literature. The smallest theoretically predicted trianion is the ionic $\text{Li}_2\text{F}_5^{3-}$ system,²⁷ which is strongly related to the discussed LiF_3^{2-} dianion. Its stability can be analogously understood in terms of electrostatic arguments. Besides this outstanding small trianion, highly negatively charged alkali metal halide chains, e.g., $\text{K}_8\text{F}_{14}^{6-}$,²⁸ and huge trianionic metal clusters, e.g., Au_{54}^{3-} ,²⁹ are known.

Recently, Wang et al. examined the tetraanion of copper phthalocyanine tetrasulfonate by measuring its photoelectron spectrum (PES).^{30,31} They used the electrospray ionization technique to generate the free anions, and after mass selection, the negative ions were intercepted by a laser beam, and the kinetic energy of the photodetached electron was measured with a magnetic-bottle photoelectron analyzer.³² In this experiment Wang et al. made a spectacular observation: they obtained a peak in the PES corresponding to a negative electron binding energy; i.e., the electrons of the highest occupied molecular orbital (HOMO) are unbound. The surprisingly long lifetime of the tetraanion (the experiment takes at least 10^{-5} s) can be explained with the existence of a repulsive Coulomb barrier (RCB), which hinders the emission of an electron from the system. The RCB is a general phenomenon in multiply charged anions and its existence can be simply rationalized by the electrostatic forces that an emitted electron experiences. The short-range attraction of the nuclei and the long-range repulsion of the remaining negatively charged anion combine to a barrier potential, the RCB, through which the electron has to tunnel to leave the MCA. Although the RCB is clearly dominated by the electrostatic forces present, it is analogous to one-particle

* Corresponding author. E-mail: andreas.dreuw@tc.pci.uni-heidelberg.de.

TABLE 1: Basis Set Study for the $\text{N}(\text{BF}_3)_4^{3-}$ Trianion^a

basis set	KT	ΔSCF	$r(\text{N}-\text{B})$	$r(\text{B}-\text{F})$	$\angle(\text{N}-\text{B}-\text{F})$	$\angle(\text{B}-\text{N}-\text{B}-\text{F})$
DZ	2.788	+0.892	1.597	1.440	112.63	39.12
DZ+sp	2.813	+1.179	1.596	1.438	112.50	39.31
DZP	1.306	-0.578	1.598	1.402	112.22	40.12
DZP+sp	1.512	-0.449	1.601	1.402	112.16	40.30

^a The vertical electron detachment energies at the level of KT and ΔSCF are shown together with the corresponding SCF optimized geometric parameters. Due to the large system size, we have to restrict ourselves to the use of basis sets of double- ζ quality.

scattering potentials a nonlocal energy-dependent potential that can be formally exactly evaluated in the framework of the Green's function formalism of scattering.³³

Returning to the tetraanion of copper phthalocyanine tetrasulfonate, it is at first glance surprising that the HOMO of this system is located in the inner region of the planar system and not at the four negatively charged sulfonate groups that are fixed at the edge of the molecule.^{30,31} At closer inspection it becomes clear that the electrons of the π -system of the inner part experience the electrostatic repulsion of four negatively charged ligands and are strongly shifted upward in energy. Therefore, the unbound electrons in the PES stem from the inner region of the molecule and, in the case of an in-plane emission, are prevented from being emitted by the repulsion of the negatively charged sulfonate groups. However, the electrons can and probably will be emitted perpendicular to the planar molecule, thus avoiding the sulfonate groups and passing a much smaller RCB potential.

In this communication, we address the question whether it is possible to find a three-dimensional analogous metastable system in which an electron is held back from emission by negative charges in all directions equally. Such a system must be spherically symmetric, the HOMO must be located in the inner region of the molecule and the negative charges have to be on the outermost shell of the sphere. We are going to show with the help of high-level ab initio methods that the $\text{N}(\text{BF}_3)_4^{3-}$ trianion possesses all these requirements and is the first long-lived *small* covalent trianion in the literature, which has been predicted theoretically or detected experimentally.

2. Computational Details

The computer programs used for our calculations stem from the GAUSSIAN98³⁴ and the GAMESS³⁵ packages. Our calculations comprise the optimization of the geometry of the $\text{N}(\text{BF}_3)_4^{3-}$ trianion and the calculation of the binding energies of the excess electrons as well as the determination of possible fragmentation channels at various levels of theory.

The data at the independent particle level were obtained using the standard self-consistent field (SCF) restricted Hartree–Fock method for the closed-shell $\text{N}(\text{BF}_3)_4^{3-}$ trianion and restricted open-shell Hartree–Fock technique for the corresponding open-shell dianion. The calculations employed the Cartesian Gaussian-type double- ζ (DZ) basis set comprising Dunning's contractions^{36,37} of Huzinaga's primitive sets.³⁸ To explore the influence of the size of the basis set on the results of our calculations, we have performed a basis set study on $\text{N}(\text{BF}_3)_4^{3-}$ at the theoretical level of HF. Due to the size of the investigated system and the need to perform high-level ab initio calculations beyond HF, we have restricted ourselves to the use of basis sets of double- ζ quality.

The basis set study (Table 1) has revealed the importance of the use of polarization functions, since the addition of the d-type polarization function leads to a shortening of the B–F bond

length of about 0.04 Å. This tremendous decrease of the size of the trianion, which causes an increase of the electrostatic repulsion between the excess negative charges, effects a strong electronic destabilization of the trianion, i.e., a smaller value for the vertical electron detachment energy (EDE) when going from DZ to DZP basis sets. The use of diffuse functions leads to a weak increase of the EDE, since more diffuse basis sets can describe the characteristics of the higher negatively charged species more accurately than basis sets without additional diffuse functions. The coefficients of the added diffuse s- and p-type functions are 0.0277 and 0.0190 for boron, 0.0619 and 0.0480 for nitrogen, and 0.0984 and 0.0740 for fluorine, respectively. In general, the bond angles and overall geometric appearance of the system is barely affected by the use of different basis sets. Larger basis sets with an even greater number of diffuse functions can of course much better describe the diffuse orbitals of the trianion, and hence their application in our calculations would yield an increased electronic stability of the system. Therefore, our calculated values represent lower bounds to the electron detachment energy and, if the system is found to be stable using the DZP+sp basis set, it is even more stable using larger and more diffuse basis sets, such as, e.g., AUG-cc-pVTZ. On the basis of our experience with the theoretical examination of smaller dianionic systems (see for example refs 15 and 18) and the size of the examined trianion, the DZP+sp basis set seems to be a useful compromise between size of the basis and calculation time. We therefore use the DZP+sp basis set as standard in our calculations, unless we explicitly mention the use of different basis sets.

Electron correlation effects were included by means of Møller–Plesset perturbation theory of second order (MP2), coupled cluster doubles (CCD),³⁹ coupled cluster singles plus doubles (CCSD),^{40,41} and the outer-valence Green's function (OVGF)^{42,43} approach. In all these correlated calculations the 1s electrons of boron, nitrogen, and fluorine were frozen and the virtual counterparts discarded.

The electron detachment energy of the $\text{N}(\text{BF}_3)_4^{3-}$ system can be obtained in two principally different ways. On one hand, there are the so-called “direct” methods, of which we have employed Koopman's theorem (KT) and the OVGF approach. While KT relates the orbital energy obtained with a closed-shell RHF calculation directly to the electron detachment energy, OVGF considers electron correlation and orbital relaxation effects. Thus, this method yields an improved electron detachment energy compared with KT. On the other hand, one can compute the EDE “indirectly” by subtracting the total energies of the dianion and the trianion. These methods are also referred to as Δ -methods. We have employed ΔSCF , ΔMP2 , ΔCCD , and ΔCCSD . Note that a positive EDE indicates that energy has to be applied to detach an electron; i.e., the system is stable with respect to electron autodetachment.

3. Geometries and Energetics of $\text{N}(\text{BF}_3)_4^{3-}$

From previous examinations of several stable gas-phase dianions we have learned that the most stable small dianions possess a positively charged central atom surrounded by equivalent, negatively charged electron affine ligands, e.g., LiF_3^{2-} ,¹⁰ BeF_4^{2-} ,^{11,12} C_7^{2-} ,¹⁵ or SiC_6^{2-} .^{17,18} For the construction of a higher negatively charged molecular system, it thus makes sense to place a positively charged center atom in the central position as well and surround it by several negatively charged groups. We have chosen nitrogen as the central atom, because the system should be spherically symmetric and nitrogen is usually tetrahedrally coordinated when it is singly positively

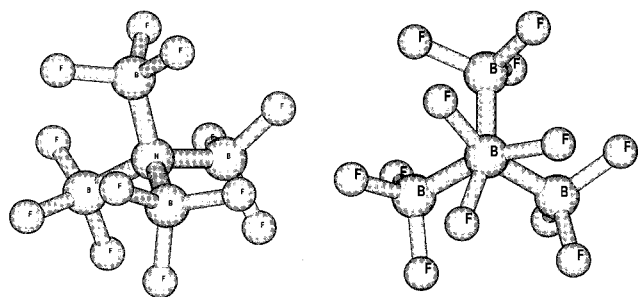


Figure 1. Structure of the T symmetric $\text{N}(\text{BF}_3)_4^{3-}$ trianion is shown in side view (left part) and along one of the four C_3 axes of the molecule (right part), where the rotation of the BF_3 units around the C_3 axes of the molecule by about 40° can be easily recognized.

TABLE 2: Geometric Parameters of the Trianion $\text{N}(\text{BF}_3)_4^{3-}$, Which Have Been Optimized at the Theoretical Levels of RHF and MP2 Using the DZP+sp Basis Set^a

	RHF	MP2
geometry		
$r(\text{N}-\text{B})$	1.599	1.603
$r(\text{B}-\text{F})$	1.402	1.427
$\angle(\text{N}-\text{B}-\text{F})$	112.12	111.98
$\angle(\text{B}-\text{N}-\text{B}-\text{F})$	40.16	40.12
EDE		
vertical		
KT	+1.514	+1.815
KT*	+1.304	+1.611
ΔSCF	-0.449	-0.112
ΔSCF^*	-0.782	-0.236
ΔMP2	-0.097	+0.170
ΔMP2^*	-0.441	-0.177
ΔCCD^*	-0.384	-0.100
ΔCCSD^*	-0.593	-0.325
OVGF^*	-0.522	-0.262

^a The bond lengths are in ångströms and the angles in degrees. The vertical electron detachment energies have been calculated for both optimized geometries using the DZP+sp basis set and the DZP basis set (*) and are given in electronvolts.

charged. Furthermore, we have added four BF_3 ligands to the central nitrogen cation, where each boron atom should be formally singly negatively charged in a tetrahedral coordination sphere. Summing up the electrons and charges, we end up with a triply negatively charged molecule (four negative boron atoms and one positive nitrogen atom), which possesses a closed-shell electronic ground state and spherical tetrahedral symmetry.

The geometry optimizations of this system at the levels of RHF as well as MP2 have shown that the system does not belong to the T_d point group but is T symmetric, since all BF_3 units are rotated about 40° along the four C_3 axis of the system, thus disturbing the higher T_d symmetry (Figure 1). Since the system is closed-shell, i.e., the triply degenerate HOMO is completely occupied, the electronic ground state is 1A_1 . As one would expect, the central nitrogen–boron bonds as well as the outer boron–fluorine bonds possess mainly covalent single bond character due to the typical bond lengths of 1.603 (1.599) and 1.427 (1.402) Å at the MP2 (SCF) level of theory, respectively (Table 2). The N–B–F bond angle has a value of about 112° at both levels of theory, which is slightly larger than the tetrahedral angle. The increase of this angle can be explained with the steric hindrance of the BF_3 units, which is, along with the electrostatic repulsion between the partly negatively charged fluorine atoms, the reason for the rotation of about 40° of the BF_3 groups out of T_d symmetry. The structure of the $\text{N}(\text{BF}_3)_4^{3-}$ trianion (Figure 1) represents a true minimum on the potential

energy surface, since an analysis of the harmonic frequencies has given only real values at the SCF level as well as at the MP2 level of theory.

The electronic stability of the system is examined by computing the vertical electron detachment energy (EDE). Using the SCF optimized geometry of the dianion and the DZP+sp basis set for the calculation of the vertical EDE, it possesses values of +1.514, -0.449, and -0.097 eV at the theoretical levels of KT, ΔSCF , and ΔMP2 , respectively (Table 2). Turning to highly correlated methods, only the DZP basis set without diffuse functions has been applied due to the size of the system. At the ΔCCD , ΔCCSD , and OVGF level, the vertical EDE is -0.384, -0.593, and -0.522 eV, respectively, and is expected to increase if a diffuse basis set could be used. Taking the average stabilization of the EDE of about 0.2 eV by the diffuse basis functions at the lower levels of theory into account (see Table 2), the system is unstable with respect to electron autoejection at the SCF optimized geometry by about -0.3 eV.

If the vertical EDE of $\text{N}(\text{BF}_3)_4^{3-}$ is calculated at the MP2 optimized geometry, it increases by about 0.3 eV at all levels of theory. Thus, the vertical EDE has values of +0.17 eV at the ΔMP2 level using the DZP+sp basis set and -0.100, -0.325, and -0.262 eV at the highly correlated levels of ΔCCD , ΔCCSD , and OVGF, respectively, with the DZP basis set. Again, if we assume a stabilization of the latter numbers by the use of diffuse basis functions within the calculations of about 0.2 eV, the vertical EDE has a value of approximately zero for the $\text{N}(\text{BF}_3)_4^{3-}$ trianion. The electronic stabilization of the trianion from the SCF to the MP2 optimized geometry is due to the elongation of the B–F bond length at the MP2 level. The longer B–F bonds lead to a spatial expansion of the molecule and a decrease of the electrostatic repulsion between the excess charges, i.e., an electronic stabilization of the trianion. A similar effect has been observed within the basis set study in section 2, when polarization functions have been introduced into the basis sets to optimize the geometry of the trianion.

A further property a stable gas-phase MCA must possess is stability with respect to fragmentation into two typically monoanionic fragments. This fragmentation is energetically favored because the monoanionic fragmentation products electrostatically repel each other strongly. The examination of different possible dissociation pathways, for instance, the dissociation into $\text{N}(\text{BF}_3)_2(\text{BF}_2)^{2-}$ and BF_4^- or into $\text{N}(\text{BF}_3)_3(\text{BF}_2)^{2-}$ and F^- , has shown that the latter is the energetically most favorable due to the high stability of the fluorine anion. Moreover, within the first dissociation process two bonds have to be broken, whereas only one B–F bond has to be broken to split off one fluorine anion.

Calculations of the sum of the total energies of the separately optimized $\text{N}(\text{BF}_3)_3(\text{BF}_2)^{2-}$ dianion and F^- reveal that the $\text{N}(\text{BF}_3)_4^{3-}$ trianion is thermodynamically unstable with respect to fragmentation into these fragments by about 2.95 eV at the level of MP2. For this reason, the energy barrier connected with this fragmentation channel has to be calculated explicitly. Since the examined trianionic system is large, only SCF and MP2 calculations are feasible to estimate the barrier height in the region of the equilibrium geometry where the single determining character of the system is guaranteed. The calculated energy barriers at these levels of theory are displayed in Figure 2 and possess values of about 1.5 eV. A similar situation has been found previously for the BeF_4^{2-} system. This system is also thermodynamically unstable with respect to fragmentation into BeF_3^- and F^- by about 3.5 eV.^{11,12} The energy barrier connected with this fragmentation channel of BeF_4^{2-} has a height of only

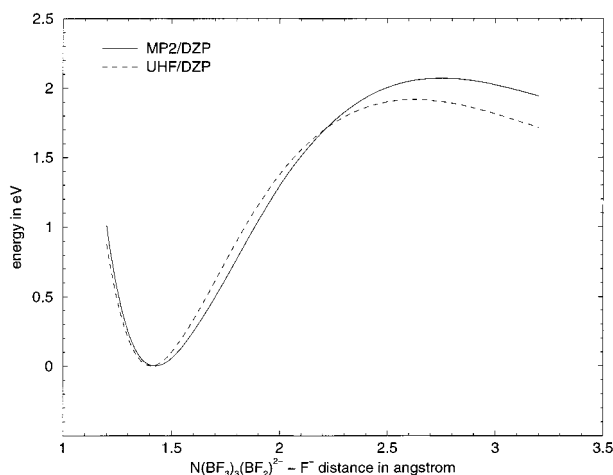


Figure 2. Dissociation pathway of $\text{N}(\text{BF}_3)_4^{3-}$ into $\text{N}(\text{BF}_3)_3(\text{BF}_2)^{2-}$ and F^- , which is the energetically most favorable dissociation channel. All geometric parameters have been separately optimized along the path.

0.6 eV, i.e., less than half of the barrier of the $\text{N}(\text{BF}_3)_4^{3-}$ trianion. However, BeF_4^{2-} has recently been observed experimentally,¹³ which makes us sure that $\text{N}(\text{BF}_3)_4^{3-}$ is also extremely long-lived with respect to dissociation. In contrast to neutral systems, the energy barrier connected with the dissociation of a multiply charged anion is very broad. The broadness of the barrier emerges through the electrostatic repulsion between the anionic dissociation products. Thus, MCAs often possess very long lifetimes with respect to dissociation, although the height of the corresponding energy barrier is moderate.

In summary, the molecular $\text{N}(\text{BF}_3)_4^{3-}$ system is long-lived with respect to dissociating and may be slightly unstable with respect to electron emission. But, as already mentioned in the Introduction, there exists a repulsive Coulomb barrier that hinders the electron from being emitted and through which the outgoing electron must tunnel. Due to this tunneling process, the $\text{N}(\text{BF}_3)_4^{3-}$ trianion is probably metastable and possesses a finite lifetime. In the next section, we will calculate a local approximation to the RCB potential that the outgoing electron experiences and estimate the corresponding tunneling lifetime in the framework of semiclassical WKB (Wentzel–Kramers–Brillouin) theory.

4. Electron Emission from $\text{N}(\text{BF}_3)_4^{3-}$

The emission of one of the excess electrons from a multiply charged anion (MCA) is always hindered by a repulsive Coulomb barrier (RCB). The RCB is a general phenomenon in MCAs and emerges through the combination of the short-range binding of the excess electrons and the long-range repulsion between the emitted electron and the remaining anion. We have shown in a previous publication, that the RCB is a complicated nonlocal and energy-dependent potential, which is not straightforward to compute.³³ A formally exact theory for the RCB exists, which is based on the Green's function formalism of scattering. Approximation schemes to determine local RCB potentials are available. It has been shown that the local potentials are reasonable estimates for the true RCB, when the system under investigation is spatially extended.³³

Here, we have employed the DFOSA (dianion's frozen orbitals static approximation) approach to calculate a three-dimensional local RCB potential. Within this approach the molecular orbitals of the trianion obtained from a closed-shell Hartree–Fock calculation are used, and one electron from the

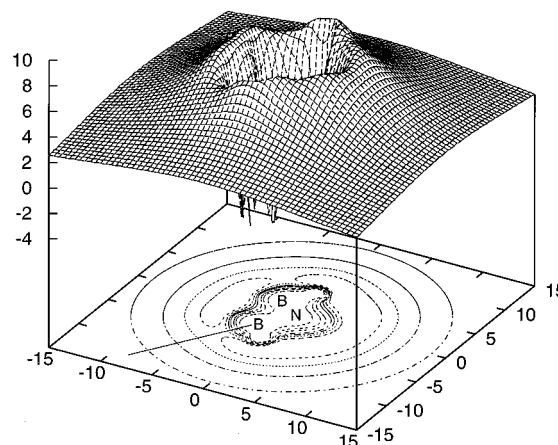


Figure 3. Two-dimensional picture of the local RCB potential of $\text{N}(\text{BF}_3)_4^{3-}$ that has been calculated in the framework of the DFOSA approach. The RCB is the potential experienced by an electron through its interaction with the residual monoanion. Altogether, there are four symmetry equivalent minimum energy paths for electron emission, which are along the four C_3 axes of the molecule. One of them is drawn as a straight line onto the projection of the potential in the xy plane. The energy is given in electronvolts and the lengths are given in angstroms.

highest occupied orbital is taken out. Then the electrostatic potential is computed by summing up the nucleus–electron attraction and electron–electron repulsion via the equation

$$V_{\text{DFOSA}}(r) = - \sum_{\alpha=1}^K \frac{Z^\alpha}{|r - r_\alpha|} + \sum_{i=1}^{N-1} \int \frac{\phi_i^* \phi_i}{|r - r_i|} dr_i$$

In this equation the first term describes the electrostatic attraction between K nuclei and the outgoing electron while the second term corresponds to the electrostatic repulsion between the outgoing electron and the remaining $N - 1$ electrons in their molecular orbitals of the trianion. A two-dimensional cut through the obtained three-dimensional RCB of the $\text{N}(\text{BF}_3)_4^{3-}$ trianion is displayed in Figure 3. The cut is made along a plane, which is given by the nitrogen and two boron atoms and embodies two minimum energy paths for electron emission. Due to the high symmetry of the system there exist four equivalent minimum energy pathways for electron emission, which are along the four C_3 axes of the molecule and point onto the boron atoms. One minimum energy path is exemplarily plotted on the horizontal projection of the potential in Figure 3.

To estimate the lifetime of the $\text{N}(\text{BF}_3)_4^{3-}$ trianion, we have used the DFOSA potential to calculate the tunneling lifetime of an electron through the RCB along the minimum energy path for electron emission (Figure 4). The calculations have been performed in the framework of the semiclassical WKB method. The tunneling probability is given by the formula

$$P = \exp \left[- \frac{2}{\hbar} \int_{r_1}^{r_2} \sqrt{2m(E - V(r))} dr \right]$$

where E is the energy of the electron, $V(r)$ is the RCB and r_1 and r_2 define the width of the barrier at energy E . The lifetime of the trianion can finally be calculated using the formula

$$\tau = \frac{2\pi}{P\omega}$$

where ω is the frequency with which the electron hits the RCB. The frequency ω is obtained by solving the equation of motion

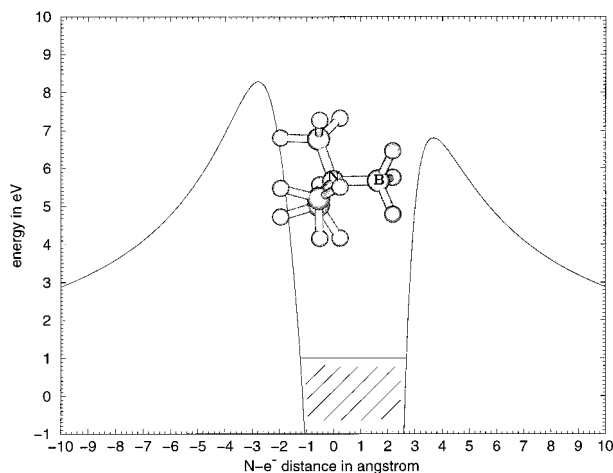


Figure 4. One-dimensional cut through the RCB of $\text{N}(\text{BF}_3)_4^{3-}$ along the minimum energy path for electron emission. The RCB has been calculated with the DFOSA method. The zero-point of the x -axis corresponds to the nitrogen atom and for a better orientation the $\text{N}(\text{BF}_3)_4^{3-}$ trianion is displayed in the length scale of the potential. For electron energies below 1 eV (corresponding to an electron detachment energy of -1 eV) the trianion has been found to live longer than $5 \mu\text{s}$, which is the minimum lifetime for a mass spectrometric observation.

for the electron with the assumption that the inner region of the RCB potential is dominated by the electrostatic attraction between the nuclei and the outgoing electron and has the shape of r^{-1} . The reliability of the obtained lifetimes and the usefulness of such simple approaches has been documented before by several groups.^{21–23,33,44}

Using this semiclassical one-dimensional approach, we have calculated the lifetime of the $\text{N}(\text{BF}_3)_4^{3-}$ system as a function of the energy of the outgoing electron. We have found that for electron energies below 1 eV (corresponding to an EDE of -1 eV) the tunneling lifetime along the minimum energy path is longer than 10^{-5} s, which is the lower limit for experimental observation in a mass spectrometer (Figure 4). In section 3 we have seen that the vertical electron detachment energy for $\text{N}(\text{BF}_3)_4^{3-}$ (Table 2) is close to zero, and for an EDE of -0.1 eV the calculated lifetime is on the order of 10^{15} s. For this reason, the trianion is long-lived with respect to electron emission and should be observable in a mass spectrometric experiment.

For this special spherical $\text{N}(\text{BF}_3)_4^{3-}$ trianion the long lifetime with respect to electron emission can be rationalized by the excess electrons hindered from emission by a sphere of negative charges. To back this claim, we must first ensure that the excess electrons are localized in the inner region of the trianion. Therefore, we examine the triply degenerate highest occupied molecular orbital (HOMO) in detail, from which an excess electron should be emitted. All three triply degenerate HOMO orbitals have the same appearance and, as an example, one of them is shown in Figure 5. The HOMO has its major coefficients at the central nitrogen atom but also has small parts on the outer fluorine atoms. In contrast, the coefficients at the boron atoms are negligible. On the basis of these grounds, we can assume that the electrons of the HOMO are primarily localized in the inner region of the spherical molecule.

The analysis of the charge distribution of this unique $\text{N}(\text{BF}_3)_4^{3-}$ molecule with the approach of Merz, Singh, and Kollman^{45,46} and Breneman and Wiberg⁴⁷ has proven that the bulk of negative charges are clearly located on the outer fluorine sphere of the molecule. While the central nitrogen atom is slightly negatively charged with a partial charge of -0.1 , the

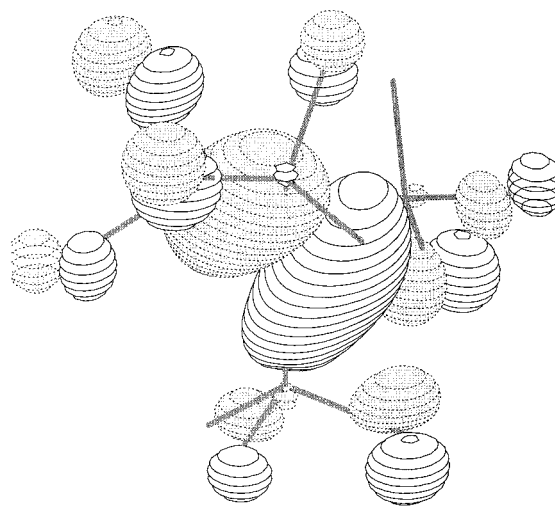


Figure 5. One of the triply degenerate highest occupied molecular orbitals of $\text{N}(\text{BF}_3)_4^{3-}$. The by far largest coefficients of this orbital are located in the center of the molecule. All three HOMO orbitals have the same spatial appearance.

boron atoms are clearly positive with about $+0.95$ and each fluorine atom carries a negative partial charge of -0.56 . In summary, a negative charge of about -7 is located on the outer shell of the molecule and a charge of $+4$ is distributed over the inner region, where the unbound electrons are mainly located. Thus, the system reflects indeed the above drawn picture of unbound electrons held back from emission by a negatively charged sphere of fluorine atoms.

5. Brief Summary

In this communication we have presented our ab initio results for the unique trianion $\text{N}(\text{BF}_3)_4^{3-}$ and have predicted its existence. The $\text{N}(\text{BF}_3)_4^{3-}$ trianion is, to our best knowledge, the first *small* long-lived covalent gas-phase trianion. In contrast to the outstanding long-lived $\text{Li}_2\text{F}_5^{3-}$, which has only purely ionic bonds, the $\text{N}(\text{BF}_3)_4^{3-}$ trianion possesses much covalent character. We have shown with the help of ab initio methods that the T symmetric system $\text{N}(\text{BF}_3)_4^{3-}$ is long-lived with respect to fragmentation of the nuclear framework. The computation of the electron detachment energy of the system revealed that it is metastable with respect to electron autoejection, since the EDE has been found to be slightly negative at highly-correlated levels of theory. To estimate the lifetime of the trianion with respect to electron autoejection, we have computed the repulsive Coulomb barrier, which an outgoing electron has to pass. For this calculation we have employed the DFOSA (dianion's frozen orbital static approximation) approach, which yields a reliable local RCB approximation. Using this ab initio calculated RCB potential, we have computed the tunneling lifetime depending on the energy of the outgoing electron in the framework of semiclassical WKB theory. We could show that the lifetime of the trianion is definitely longer than $5 \mu\text{s}$, which is the lower limit for an observation in a mass spectrometric experiment.

An analysis of the charge distribution has shown that the structure of the $\text{N}(\text{BF}_3)_4^{3-}$ trianion can be seen as a slightly negatively charged nucleus (the nitrogen atom) surrounded by a sphere of four positive charges (the four boron atoms), which is again enveloped in a sphere of seven negative charges (distributed over the terminal twelve fluorine atoms), building up a sequence of differently charged spheres that stabilize each

other. The excess three negative charges of the trianion are strongly stabilized by the succession of negative and positive charges.

Finally, we would like to stress that the RCB exists in every multiply charged anion (MCA) and hinders the emission of one of the excess electrons. The special feature of the $\text{N}(\text{BF}_3)_4^{3-}$ trianion that the HOMO is localized in the inner region of the molecule and an outgoing electron has to pass a sphere of negative charges helps stabilize the trianion but is not a general requirement for the existence of the RCB. In contrast, most of the free long-lived MCAs, e.g., BeC_4^{2-} ,^{20,21} possess HOMOs that are localized in the outer region of the molecule, but nonetheless, there is also a RCB for these systems. The reason is that the RCB emerges only by the electrostatic repulsion between the emitted electron and the remaining anion, which is independent from where the HOMO of the original MCA is localized.

References and Notes

- (1) Janoschek, R. Z. *Anorg. Allg. Chem.* **1992**, 616, 101.
- (2) Scheller, M. K.; Cederbaum, L. S. *J. Phys. B* **1992**, 25, 2257.
- (3) Sommerfeld, T. *J. Phys. Chem. A* **2000**, 104, 8806.
- (4) Boldyrev, A. I.; Simons, J. *J. Phys. Chem.* **1994**, 98, 2298.
- (5) McKee, M. L. *J. Phys. Chem.* **1996**, 100, 3473.
- (6) Blades, A. T.; Kebarle, P. *J. Am. Chem. Soc.* **1994**, 116, 10761.
- (7) Kalcher, J.; Sax, A. F. *Chem. Rev.* **1994**, 94, 2291.
- (8) Scheller, M. K.; Compton, R. N.; Cederbaum, L. S. *Science* **1995**, 270, 1160.
- (9) Freeman, G. R.; March, N. H. *J. Phys. Chem.* **1996**, 100, 4331.
- (10) Scheller, M. K.; Cederbaum, L. S. *J. Chem. Phys.* **1993**, 99, 441.
- (11) Weikert, H. G.; Cederbaum, L. S.; Tarantelli, F.; Boldyrev, A. I. *Z. Phys. D—Atoms, Molecules Clusters* **1991**, 18, 229.
- (12) Weikert, H. G.; Cederbaum, L. S. *J. Chem. Phys.* **1993**, 99, 8877.
- (13) Middleton, R.; Klein, J. *Phys. Rev. A* **1999**, 60, 3515.
- (14) Schauer, S. N.; Williams, P.; Compton, R. N. *Phys. Rev. Lett.* **1990**, 65, 625.
- (15) Sommerfeld, T.; Scheller, M. K.; Cederbaum, L. S. *Chem. Phys. Lett.* **1993**, 209, 216.
- (16) Berghof, V.; Sommerfeld, T.; Cederbaum, L. S. *J. Phys. Chem. A* **1998**, 102, 5100.
- (17) Dreuw, A.; Sommerfeld, T.; Cederbaum, L. S. *Angew. Chem., Int. Ed. Engl.* **1997**, 36, 1889.
- (18) Dreuw, A.; Sommerfeld, T.; Cederbaum, L. S. *J. Chem. Phys.* **1998**, 109, 2727.
- (19) Gnaser, H. *Phys. Rev. A* **1999**, 60, R2645.
- (20) Klein, J.; Middleton, R. *Nucl. Instrum. Methods Phys. Res. B* **1999**, 159 (1–2), 8–21.
- (21) Dreuw, A.; Cederbaum, L. S. *J. Chem. Phys.* **2000**, 112, 7400.
- (22) Wang, X.-B.; Wang, L.-S. *Phys. Rev. Lett.* **1999**, 83, 3402.
- (23) Weis, P.; Hampe, O.; Gilb, S.; Kappes, M. M. *Chem. Phys. Lett.* **2000**, 321, 426.
- (24) Dewar, M.; Zoebisch, E.; Healy, E.; Stewart, J. J. *Am. Chem. Soc.* **1985**, 107, 3902.
- (25) Maas, W. P. M.; Nibbering, N. M. M. *Int. J. Mass Spectrom. Ion Processes* **1989**, 88, 257.
- (26) Wang, L.-S.; Ding, C.-F.; Wang, X.-B.; Nicholas, J. B. *Phys. Rev. Lett.* **1998**, 81, 2667.
- (27) Scheller, M. K.; Cederbaum, L. S. *J. Chem. Phys.* **1994**, 100, 8943.
- (28) Scheller, M. K.; Cederbaum, L. S. *J. Chem. Phys.* **1994**, 101, 3962.
- (29) Yannouleas, C.; Landmann, U.; Herlett, A.; Schweikhard, L. *Phys. Rev. Lett.* **2001**, 86, 2996.
- (30) Wang, X.-B.; Wang, L.-S. *Nature* **1999**, 400, 245.
- (31) Wang, X.-B.; Ferris, K.; Wang, L.-S. *J. Chem. Phys.* **2000**, 104, 25.
- (32) Wang, L.-S.; Ding, C.-F.; Wang, X.-B. *Rev. Sci. Instrum.* **1999**, 70, 1957.
- (33) Dreuw, A.; Cederbaum, L. S. *Phys. Rev. A* **2001**, 63, 012501. Due to production errors, see Erratum: *Phys. Rev. A* **2001**, 63, 049904.
- (34) Frisch, M. J.; Trucks, G. W.; Schlegel, H. B.; Scuseria, G. E.; Robb, M. A.; Cheeseman, J. R.; Zakrzewski, V. G.; Montgomery, J. A., Jr.; Stratmann, R. E.; Burant, J. C.; Dapprich, S.; Millam, J. M.; Daniels, A. D.; Kudin, K. N.; Strain, M. C.; Farkas, O.; Tomasi, J.; Barone, V.; Cossi, M.; Cammi, R.; Mennucci, B.; Pomelli, C.; Adamo, C.; Clifford, S.; Ochterski, J.; Petersson, G. A.; Ayala, P. Y.; Cui, Q.; Morokuma, K.; Malick, D. K.; Rabuck, A. D.; Raghavachari, K.; Foresman, J. B.; Cioslowski, J.; Ortiz, J. V.; Stefanov, B. B.; Liu, G.; Liashenko, A.; Piskorz, P.; Komaromi, I.; Gomperts, R.; Martin, R. L.; Fox, D. J.; Keith, T.; Al-Laham, M. A.; Peng, C. Y.; Nanayakkara, A.; Gonzalez, C.; Challacombe, M.; Gill, P. M. W.; Johnson, B. G.; Chen, W.; Wong, M. W.; Andres, J. L.; Head-Gordon, M.; Replogle, E. S.; Pople, J. A. *Gaussian 98*, revision A.7; Gaussian, Inc.: Pittsburgh, PA, 1998.
- (35) Schmidt, M. W.; Boatz, J. A.; Baldridge, K. K.; Koseki, S.; Gordon, M. S.; Elbert, S. T.; Lam, B. *QCPE Bull.* **1987**, 7, 115.
- (36) Dunning, T. H., Jr. *J. Chem. Phys.* **1970**, 53, 2823.
- (37) Dunning, T. H., Jr. *J. Chem. Phys.* **1971**, 55, 716.
- (38) Huzinaga, S. *J. Chem. Phys.* **1965**, 42, 1293.
- (39) Bartlett, R. J.; Purvis, G. D., III. *Int. J. Quantum Chem.* **1978**, 14, 561.
- (40) Purvis, G. D., III; Bartlett, R. J. *J. Chem. Phys.* **1982**, 76, 1910.
- (41) Bartlett, R. J. *J. Phys. Chem.* **1989**, 93, 1697.
- (42) Cederbaum, L. S. *J. Phys. B* **1975**, 8, 290.
- (43) von Niessen, W.; Schirmer, J.; Cederbaum, L. S. *Comput. Phys. Rep.* **1984**, 1, 57.
- (44) Simons, J.; Skurski, P.; Barrios, R. *J. Am. Chem. Soc.* **2000**, 122, 11893.
- (45) Besler, B. H.; Merz, K. M.; Kollmann, P. A. *J. Comput. Chem.* **1990**, 11, 431.
- (46) Singh, U. C.; Kollmann, P. A. *J. Comput. Chem.* **1984**, 5, 129.
- (47) Breneman, C. M.; Wiberg, K. B. *J. Comput. Chem.* **1990**, 11, 361.